Journal of Marine Research, 54, 939–966, 1996

An experimental and modeling study of pH and related solutes in an irrigated anoxic coastal sediment

by Roberta L. Marinelli[1] and Bernard P. Boudreau[2]

ABSTRACT

Macrofaunal irrigation is an important process in nearshore sediments, facilitating greater exchange between sediments and seawater and imparting significant lateral heterogeneity to the porewater profiles of many constituents. Like many macrofaunal activities, irrigation is a transient behavior, i.e. tubes and burrows are flushed periodically, at frequencies that generally are species-specific. As a result, transient concentrations within the dwelling arise, potentially impacting gradients, fluxes and reaction rates in the vicinity of the dwelling. We investigated the impact of periodic burrow irrigation on the distribution of several diagenetically important porewater constituents. Laboratory experiments evaluated irrigation periodicity using artificially irrigated tubes embedded in nearshore organic-rich sediments, and microdistributions of oxygen and pH in laboratory experiments were measured with microelectrodes. To help interpret our results, we also constructed a simplified time and space-dependent transport-reaction model for oxygen, pH and sulfide in irrigated sediments.

Laboratory results show substantial differences in the pH field of sediments surrounding an irrigated tube as a function of irrigation frequency. Higher pH values, indicative of an overlying water signature, were observed in the vicinity of the tube wall with increasing duration of irrigation. Conversely, oxygen concentrations did not vary significantly with the amount of irrigation, most likely a result of extremely high sediment oxygen demand. Model results are consistent with laboratory findings in predicting differences in the measured variables as a function of irrigation frequency. However, the nature and extent of the model-predicted differences are often at variance with the experimental data. Overall, experimental and modeling results both suggest irrigation periodicity can substantially influence porewater distributions and diagenetic processes in sediments. Future studies should examine the influence of irrigation periodicity on the types and rates of reactions, and the attendant biological features, in the environment encompassing the tube or burrow wall.

1. Introduction

The influence of macrofauna on sediment geochemical properties of coastal, estuarine and continental shelf environments is significant. Sediments and associated organic matter are mixed and altered through burrowing, ingestion, and construction of temporary and permanent dwellings (e.g. Aller, 1978; Aller and Yingst, 1985; Wheatcroft *et al.,* 1994).

1. Skidaway Institute of Oceanography, 10 Ocean Science Circle, Savannah, Georgia, 31411, U.S.A.
2. Department of Oceanography, Dalhousie University, Halifax, Nova Scotia, Canada, B3H 4J1.

Solute gradients are steepened, and fluxes are enhanced during irrigation and burrowing (Aller, 1982; Marinelli, 1992; Martin and Banta, 1992). These activities impart a multidimensional heterogeneity to the sediment matrix, imposing both spatial and temporal variability in gradients over a range of length and time scales (Kristensen *et al.,* 1991; Krager and Woodin, 1993). Ultimately, they can affect the overall rate of diagenetic reactions, in particular, the rate of organic matter decomposition and carbon burial (Kristensen and Blackburn, 1987), as well as ecological processes, including activities and distributions of macrofauna and meiofauna (e.g. Woodin, 1984, 1985; Meyers *et al.,* 1987a, b; Marinelli, 1994).

In spite of the acknowledged importance of macrofauna to geochemical processes, few studies have examined the extent to which the specific and often transient (i.e. time-dependent) behaviors of macrofuna affect the three-dimensional sediment-porewater environment. Recent studies suggest that transient conditions imposed by macrofauna may profoundly affect mineralization processes and fluxes in nearshore environments. For example, experiments by Aller (1994a) show that exposure of organic matter to oscillating redox conditions, similar to those produced by periodic bioturbation, promotes storage of lysable NH_4^+ relative to purely oxic or anoxic conditions. Similarly, experiments by Marinelli (1992) suggest that transient feeding behaviors of surface deposit-feeding polychaetes on benthic diatoms produces a time-dependent flux of silicate from sediments to overlying water. These and other studies (Meyers *et al.,* 1987a, b; Forster and Graf, 1992) show that variable behaviors of different groups of macrofuna promote vastly different sedimentary conditions with distinct geochemical and biological consequences. This outcome suggests that additional consideration of the spatial and temporal scales over which specific macrofaunal activities operate is warranted.

During irrigation, large solute gradients across the tube-sediment interface develop, and fluxes across this interface are enhanced. As the vast majority of macrofauna ventilate their dwellings periodically (Wells, 1949; Wells and Dales, 1951; Dales, 1961; Mangum, 1964; Dales *et al.,* 1970; Kristensen, 1983), i.e. irrigation of the tube followed by a quiescent, nonirrigation period, transient concentrations within the dwelling arise, potentially impacting gradients, fluxes and reaction rates. An important question is whether this time-dependent activity has significant consequences for diagenetic processes in nearshore sediments.

A recent modeling study by Boudreau and Marinelli (1994) examined the theoretical impact of time-varying irrigation activity (periodic or discontinuous irrigation) on solute gradients in sediments and solute fluxes across the sediment-water interface. To simulate discontinuous irrigation, we employed a numerical version of Aller's (1980) tube model, allowing concentrations within the tube/burrow-annulus to vary with irrigation frequency.

With our model, it was possible to assess the effects of periodic or discontinuous irrigation on silica dissolution, assumed to follow first-order kinetics, and ammonium production, assumed to follow zeroth-order kinetics, as in Aller (1980). Our model results show first, that the effects of irrigational periodicity on solute profiles and fluxes varies

with the kinetic form of the reaction (zero vs. first order). Solute profiles resulting from discontinuous irrigation are substantially different from those driven by continuous irrigation for the zeroth-order reaction, but are similar for the first-order reaction. Second, the importance of irrigation periodicity varies with the radii of the tube and surrounding sediment. Greater differences between solute profiles resulting from discontinuous vs. continuous irrigation occur when the volume of surrounding sediment is small relative to the surface area of tube or burrow wall. Finally, periodic irrigation imposes a time dependence on fluxes across the burrow-sediment and sediment-water interface within a given irrigation/nonirrigation cycle. However, average fluxes over an entire irrigation/nonirrigation cycle are similar to those for continuous irrigation.

Based on the above arguments, we decided to study the distribution of three diagenetically active species now amenable to rapid microelectrode measurement, i.e. O_2, ΣH_2S and pH, in the vicinity of a continuously versus periodically irrigated tube. Boudreau (1987, 1991) and Boudreau and Canfield (1988, 1993) have already investigated the processes that can affect pH in sediments in which irrigation is unimportant or absent. They found that pH responded to the type of organic matter decomposition, the oxidation of ammonium and sulfide, the reduction of iron oxides (and probably manganese oxides as well), and the formation of iron monosulfide minerals. These processes are intimately linked to organic matter oxidation using oxygen and sulfate as oxidants; thus, O_2 and ΣH_2S are two important determinants of porewater pH. The present study provides us with the opportunity to discover the potential impact of irrigation on the complex reaction-system governing the pH of sedimentary porewaters.

Below, we present results of laboratory experiments in which we measured 3-D distributions of oxygen and pH near an artificially irrigated burrow. In addition, to help interpret our results, we constructed a simplified time and space-dependent transport-reaction model for pH in this system. While this model is not a faithful representation of the experimental system, it contains enough detail to provide considerable insight into the observed phenomena.

2. Laboratory experimental methods

a. Experimental setup. Effects of continuous and periodic irrigation on solute profiles of oxygen and pH were examined in paired laboratory cores (Fig. 1) containing natural sediments alone (control core) or with an irrigated tube (experimental core). We chose to simulate an irrigated tube rather than use real animals in experimental cores for several reasons. First, use of real macrofauna would require continuous monitoring of irrigation frequency and rate, a somewhat difficult task over a two month period. Second, manipulation of irrigation frequency would require that we use several different species of macrofauna with different irrigation behaviors in our experiments. Because the burrow and tube walls of macrofauna, both within and among species, are highly variable (e.g. Aller, 1983), it is possible to confound an "irrigation effect" with a "burrow wall effect."

The artificial irrigation system obviated many of these problems, allowing us to control

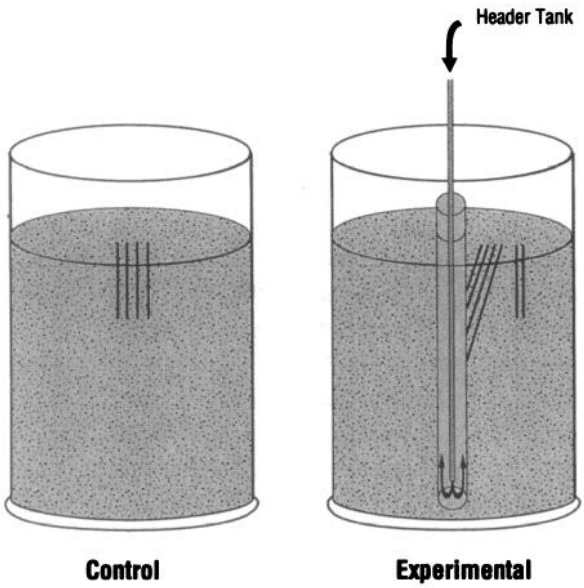

Figure 1. Schematic of experimental and control cores used in laboratory experiment. Core dimensions are 18 cm length by 11 cm diameter. Irrigation tube dimensions 15 cm length × 1 cm diameter, therefore $r_1 = 0.5$ and $r_2 = 4.2$. Location of microelectrode profiles are indicated by lines.

both irrigation frequency and the initial tube wall composition, while successfully mimicking a naturally irrigated dwelling (see Marinelli, 1994). The system consisted of a tube that was fed by a seawater-filled header tank at prescribed intervals (Fig. 1). The tube was made of three concentric layers of 0.45 μM nylon membrane, with an inner radius of 0.5 cm and length of 15 cm. The base of the tube was a solid plastic disc (blind tube), and the top portion was open. Subsequent tests of the diffusive permeability of the nylon membrane, using the methods described in Aller (1983), show that it is permeable to diffusion and that it offers a hindrance to diffusion similar to that provided by real worm tubes (0.24–0.26, within the range reported by Aller, 1983). Irrigation of the artificial tube was achieved by suspending a small diameter hollow glass tube inside the rolled nylon membrane. The glass tube was connected to a header tank such that when the header tank was filled, seawater would pass through the glass tube to the base of the artificial tube, then up along the sides and out the top (Fig. 1).

Fine-grained surficial sediments were collected from an intertidal site on the eastern side of Halifax Harbour, Nova Scotia Canada (Latitude: 44°36′N Longitude: 63°30′W), during June, 1993. The sediments are moderately well sorted, and characterized by a median grain size of 210 μm and a total sediment organic carbon content of approximately 1% (Hargrave and Phillips, 1981). The dominant macrofauna include a variety of irrigating and bioturbating organisms, such as *Arenicola marina, Mya arenaria, Macoma balthica* and *Nereis diversicolor* (Emerson and Grant, 1981 and personal observations), and during warmer

months, *Beggiatoa*-like mats have been observed at the sediment surface (Hargrave and Phillips, 1981 and personal observations). Sediments were returned immediately to a laboratory at Dalhousie University in Halifax, and were passed through a 350 μm sieve, using as little water as possible, to eliminate larger macrofauna at the site (e.g. arenicolid polychaetes). Some smaller macrofauna (e.g. spionid polychaetes), as well as meiofauna, passed through the sieve with the sediment. To eliminate all possible gradients, sediments were homogenized (by hand) and allowed to settle for several hours. Subsequently, sediments were added gradually to the control (no tube) and experimental (tube in place) plexiglass cores until the depth of the entire sediment column was approximately 18 cm. The artificial tube protruded 0.5 cm above the sediment surface. The cores were placed in a running seawater bath, with the top of the core submerged. Thus, free exchange of core overlying water with fresh seawater was permitted at all times. The system was allowed to equilibrate for several days to allow sediments to settle and gradients to begin to develop.

We tested the effects of three different irrigation frequencies on oxygen and pH gradients in sediments surrounding the tube. These frequencies fall within the range of irrigation behaviors observed in macrofauna (e.g. Wells, 1949; Wells and Dales, 1951; Dales 1961) and capture end-member and intermediate conditions. In all cases, the total cycle was one hour long, with irrigation occurring for some portion of that time. Infrequent irrigation was designated as 5 minutes of irrigation followed by 55 minutes of no irrigation. Intermediate frequency irrigation consisted of 20 minutes of irrigation followed by a 40 minute quiescent period. Continuous irrigation consisted of constant ventilation (i.e. 60 minutes out of the 60 minute cycle). Filling of the header tank for the appropriate intervals was accomplished using a peristaltic pump connected to a timer. Dye tests revealed that during irrigation, the tube was completely flushed within 10 seconds. We calculate the volume flow rate of water through the tube (excluding the portion occupied by the glass rod) to be 0.95 mls min^{-1}, a rate well within the range of flushing behaviors of a variety of tubiculous worms (Aller, 1977). This rate, divided by the cross-sectional area (the area between the edge of the burrow and the edge of the hollow tube), gives a flow velocity of 1.5 cm sec^{-1}. The pipe Reynolds number $Re = UL/v$, where

$$U = \text{flow velocity} = 1.5 \text{ cm sec}^{-1},$$

$$L = \text{cross-sectional length scale} = 0.28 \text{ cm}$$

$$v = \text{kinetic viscosity} = 0.01 \text{ cm}^2 \text{ sec}^{-1}$$

is 42. While this calculation is not strictly appropriate for an annulus, the value of the Reynolds number is approximately 50 times lower than that for the transition between laminar and turbulent flow, suggesting that flow through the artificially irrigated tube was laminar. Similar values should characterize flows through most animal tubes and burrows.

Our experimental protocol was influenced by several important considerations. First, even though sediments were homogenized and evenly distributed between the experimental and control cores, we nevertheless expected some variance in the biogeochemical

properties between cores, irrespective of irrigation frequency. Second, the microelectrode measurements were time-consuming, taking several days to complete (including measurements and calibrations) on two cores alone. Third, the recently homogenized sediments were not in steady state. These conditions prevented us from including replicates, as the time required for the microelectrode measurements would be extended, and the chemical characteristics of the core might have changed substantially between the beginning and end of the measurement period. Thus, we chose to adopt a "repeated measures approach" for conducting the experiment. This method assumes that all subjects (cores) have individual variability that may affect their response to a given treatment (irrigation frequency). If the same subject (core) is observed under different experimental conditions (allowing a sufficient amount of time between treatments), then any differences in the subject's response to the treatment is due to treatment effects, rather than experimental error (Winer, 1971).

With the repeated measures philosophy as our guide, we subjected the experimental core to the three different irrigation cycles in sequence, while allowing the control core to remain undisturbed. Our previous model results suggested that the influence of irrigation on solute profiles was most pronounced close to the burrow (e.g. $\ll$1 cm) and decayed rapidly with distance (e.g. 2 cm). Moreover, the model results indicated that sediments irrigated by a 0.5 cm radius, 15 cm deep burrow surrounded by 4 cm of sediment attained quasi-steady conditions (i.e. solute profiles were stable except for irrigation-related differences) within 10 days. Thus, we subjected the experimental core to the 5 minute irrigation cycle continually for 10 days, and subsequently made microelectrode measurements on the experimental and controls cores over the following 3–4 day period. Then, we switched to 20 minute intermediate irrigation, allowed the sediments to equilibrate under this irrigation regime for 10 days, and made the microelectrode measurements on each core over the next 3–4 days. Finally, the experimental core was irrigated continuously for 10 days, and the last set of measurements was completed. During equilibration, cores were maintained in a running seawater bath at ambient temperature (11°C). During microprofiling measurements, a core was removed from the running seawater bath and placed in a rectangular water jacket continually flushed with flowing seawater. Irrigation of the experimental core at the appropriate cycle was maintained throughout the measurement phase. The time required to complete profiles ranged from 10 to 45 minutes, varying with the constituent measured and the depth of the profile.

b. Microelectrode measurements. Our microelectrode measurements consisted of 3–4 vertical profiles at random points along a plane in the unirrigated control, ranging in depth from 0.5 cm (oxygen) to 4 cm (pH) (Fig. 1). In the experimental irrigated core, 4–5 profiles were made at an angle to the tube, always along the same plane, within the expected zone of influence of irrigation ($<$2 cm), and 2 vertical profiles were made away from this region ($>$3 cm from the tube edge) (Fig. 1). The angle profiles (0–2 cm from tube) ranged in angular depth from 1–7 cm, whereas the vertical profiles ($>$3 cm from tube edge) ranged in

depth from 0.5–4.0 cm (Fig. 1). Comparison of data from the control cores with data obtained from the sediments far from the influence of irrigation gave us a way to determine whether the control and irrigated cores were behaving similarly throughout the experiment. We also attempted to obtain microelectrode profiles of sulfide. Unfortunately, the drift in the sulfide probe was high, making it difficult to resolve the $S^{=}$ concentration, particularly in the highest concentration areas. These results will not be discussed further.

We chose to use larger diameter (1 mm or less), longer (4–10 cm) and more sturdy electrodes in our experimental study. These probes allowed us to obtain relatively fine-scale measurements of all constituents at greater depths (e.g. 6 cm) than are commonly probed with micron-tipped electrodes. The oxygen and pH electrodes were purchased from Diamond General (Ann Arbor, MI, USA). The oxygen electrode was a custom-made gold-tipped platinum sensor (0.7 mm diameter, 10 cm length) with an external Ag/AgCl reference. The electrode was calibrated in seawater of different oxygen concentrations (achieved by nitrogen bubbling) as determined by the Winkler titration. At least 4 oxygen values (including a zero value) were obtained for each calibration, and all calibration curves (concentration vs. amperage) gave $r^2 > 0.990$. The pH electrode was a combination needle electrode (1 mm diameter, 7.6 cm length) and was calibrated using commercially available buffer solutions (pH 4, 7 and 10). Calibration curves for the pH electrode gave $r^2 > 0.99$. Electrodes were calibrated at the beginning of each measurement day, and were checked in between profiles by immersion in pH solutions (pH electrode) or by additional Winkler analyses (oxygen electrode).

3. Diagenetic setting and a model

The sediments used in our experiments are strongly anoxic terrigenous muds. The Halifax Habour region has considerable primary productivity, so that virtually all muddy sediments contain >1% organic matter (and as high as 9% in Bedford Basin). The sediments we used contained enough organic matter and were sufficiently anoxic that patchy *Beggiatoa* mats developed in cores (as in the field, see Hargrave and Phillips, 1981), In such sediments one would expect that the primary electron acceptors for organic matter decay are oxygen and sulfate, i.e.

$$(CH_2O)_{106}(NH_3)_{16}H_3PO_4 + 138O_2 \rightarrow 122H_2O + 106CO_2 + 16NO_3 + 16H^+ + H_3PO_4 \quad \text{(I)}$$

$$(CH_2O)_{106}(NH_3)_{16}H_3PO_4 + 53SO_4^{=} \rightarrow 106HCO_3^- + 53H_2S + 16NH_3 + H_3PO_4 \quad \text{(II)}$$

Nitrate will be a minor oxidant. Particle-bound manganese and iron may be important when bioturbation and nonlocal particle motions are operative (Aller, 1994b; Canfield *et al.*, 1994). However, with the removal of the macrofauna, these probably play a minor role in organic matter decomposition within our experiment setup. Organic matter is assumed to have Redfield stoichiometry.

The pH of the porewaters will be buffered by the dissolved carbonate and sulfide

systems, i.e.

$$CO_{2(aq)} + H_2O \overset{K_{C1}}{\longleftrightarrow} HCO_3^- + H^+ \quad \text{(III)}$$

$$HCO_3^- \overset{K_{C2}}{\longleftrightarrow} H^+ + CO_3^= \quad \text{(IV)}$$

$$H_2S \overset{K_S}{\longleftrightarrow} H^+ + HS^- \quad \text{(V)}$$

and water itself will offer a very limited amount of buffering,

$$H_2O \overset{K_W}{\longleftrightarrow} H^+ + OH^- \quad \text{(VI)}$$

where K_{C1}, K_{C2}, K_S and K_W are the known dissociation constants for these acid-base dissociation reactions. Reactions (III) through (VI) are considered to be both reversible and fast, so that they are essentially at equilibrium at every point in the porewaters.

A large part of the sediment O_2-demand will undoubtedly be from the oxidation of reduced by-products, i.e. dissolved ammonium and sulfide. Of the two, we assume sulfide oxidation is the dominant process under strongly anoxic conditions (Boudreau and Canfield, 1993), and only these reactions are considered further,

$$H_2S + 2O_2 \rightarrow 2H^+ + SO_4^= \quad \text{(VII)}$$

$$HS^- + 2O_2 \rightarrow H^+ + SO_4^= \quad \text{(VIII)}$$

a. The model. It is our working hypothesis that reactions (I) through (VIII) are the primary determinants of the distributions of O_2, ΣH_2S and pH in our experimental porewaters. To help evaluate this hypothesis, we have constructed a multi-dimensional diagenetic (conservation) model. Our model includes the effects of (1) organic matter oxidation reactions (I) and (II), (2) the acid-base reactions (III) through (VI), and (3) sulfide oxidation reactions (VII) and (VIII). This transport-reaction model is based on the general diagenetic equation (Berner, 1980) expressed in the cylindrical coordinate system (Aller, 1980). For constant porosity, negligible adsorption and no advection, the governing equations are:

$$\frac{\partial[O_2]}{\partial t} = D_{O_2}\nabla^2[O_2] - \frac{138}{106}\frac{R_0 e^{-ax}[O_2]}{K_{O_2} + [O_2]} - 2K_{OS}[O_2]([H_2S] + [HS^-]) \quad (1)$$

$$\frac{\partial[SO_4]}{\partial t} = D_{SO_4}\nabla^2[SO_4] - \frac{1}{2}\left(\frac{R_0 e^{-ax}[SO_4]}{K_{SO_4} + [SO_4]}\right)\left(\frac{K_p}{K_p + (O_2)}\right) + K_{OS}[O_2]([H_2S] + [HS^-]) \quad (2)$$

$$\frac{\partial[CO_2]}{\partial t} = D_{CO_2}\nabla^2[CO_2] - R_{C1} + \frac{R_0 e^{-ax}[O_2]}{K_{O_2} + [O_2]} \tag{3}$$

$$\frac{\partial[HCO_3^-]}{\partial t} = D_{HCO_3^-}\nabla^2[HCO_3^-] + R_{C1} - R_{C2} + \left(\frac{R_0 e^{-ax}[SO_4]}{K_{SO_4} + [SO_4]}\right)\left(\frac{K_p}{K_p + [O_2]}\right) \tag{4}$$

$$\frac{\partial[CO_3^=]}{\partial t} = D_{CO_3^=}\nabla^2[CO_3^=] + R_{C2} \tag{5}$$

$$\frac{\partial[H_2S]}{\partial t} = D_{H_2S}\nabla^2[H_2S] + R_S + \frac{1}{2}\left(\frac{R_0 e^{-ax}[SO_4]}{K_{SO_4} + [SO_4]}\right)\left(\frac{K_p}{K_p + [O_2]}\right) - K_{OS}[O_2][H_2S] \tag{6}$$

$$\frac{\partial[HS^-]}{\partial t} = D_{HS^-}\nabla^2[HS^-] + R_S - K_{OS}[O_2][HS^-] \tag{7}$$

$$\frac{\partial[H^+]}{\partial t} = D_{H^+}\nabla^2[H^+] + R_{C1} + R_{C2} + R_S + R_W + K_{OS}[O_2](2[H_2S] + [HS^-]) \tag{8}$$

$$\frac{\partial[OH^-]}{\partial t} = D_{OH^-}\nabla^2[OH^-] + R_W \tag{9}$$

where t is time and ∇^2 is the Laplacian (diffusion) operator in cylindrical coordinates assuming radial symmetry, i.e.

$$\nabla^2[C] = \frac{\partial^2 C}{\partial x^2} + \frac{1}{r}\frac{\partial}{\partial r}\left(r\frac{\partial C}{\partial r}\right) \tag{10}$$

where x is depth and r is the radial distance, see Figure 2. D_{O_2}, D_{SO_4}, etc. are the porewater diffusion coefficients for O_2, $SO_4^=$, etc, corrected for the effects of tortuosity (see Berner, 1980). R_0 is the maximum rate of organic matter oxidation at the sediment-water interface, and "a" is a depth-attenuation constant. K_{OS} is the rate constant for sulfide oxidation. (We take this approach with the organic matter as we did not obtain data to justify its explicit modeling.) R_{C1}, R_{C2}, R_S and R_W are unknown, fast and reversible net interconversion rates for reactions (III) through (IV). K_{O_2}, K_{OS} and K_{SO_4} are saturation constants associated with Monod-type expression for oxidant utilization (Monod 1949). This expression links the rate of utilization of a constituent with its concentration, such that this rate, R, approaches zero as the concentration, C, approaches zero:

$$R = \frac{R_{max}C}{(K_C + C)} \tag{11}$$

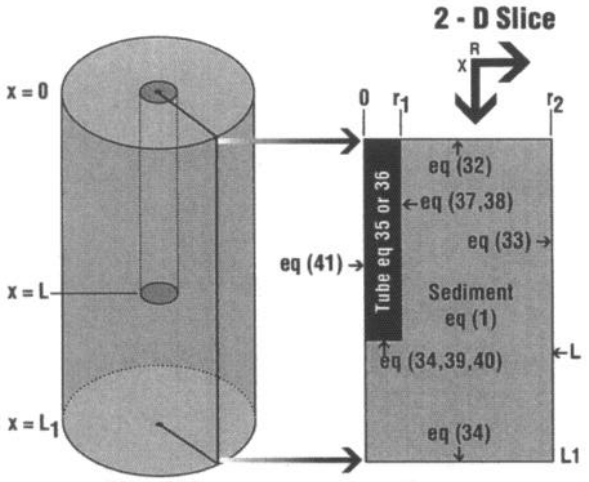

Figure 2. Schematic illustration of modified cylindrical burrow-sediment system region for the discontinuous irrigation model. Eqs. (1)–(9) describe solute conservation in the sediment region. Eq. (36) applies in the tube during nonirrigation periods, and during irrigation, $C = C_0$ (Eq. 35). The surfaces on which the boundary conditions apply, and their attendant equations in the text, also are indicated.

where K_C is the concentration at which rate is half its maximum (e.g. Boudreau and Westrich, 1984; Rabouille and Gaillard, 1991). Finally, K_p is an oxygen inhibition concentration above which the utilization of sulfate as an electron acceptor is inhibited (see Van Cappellen *et al.,* 1993).

The unknown rate terms associated with the acid-base reactions are eliminated by adding combinations of the various conservation equations (see Boudreau, 1987, 1991; Boudreau and Canfield, 1988, 1993). The reduced set of equations without these terms is underdetermined. To remove this problem, we adopt several additional equilibrium relations:

$$K_{C1}[CO_2] - [HCO_3^-][H^+] = 0 \tag{12}$$

$$K_{C2}[HCO_3^-] - [CO_3^=][H^+] = 0 \tag{13}$$

$$K_S[H_2S] - [HS^-][H^+] = 0 \tag{14}$$

$$K_W - [OH^-][H^+] = 0 \tag{15}$$

This procedure is justified by the fast reversibility of these reactions (Boudreau, 1987).

To obtain a system of equations that is amendable to standard numerical methods, we adopt the following justifiable assumptions:

$$D_{CO_2} \approx D_{HCO_3^-} \tag{16}$$

$$D_{CO_3^=} \approx D_{HCO_3^-} \tag{17}$$

$$D_{H_2S} \approx D_{HS^-} \tag{18}$$

$$D_{CO_3^=} \approx D_{HS^-} \tag{19}$$

$$D_{H^+}[H^+] \ll D_{CO_3^=}[CO_3^=] \tag{20}$$

$$D_{H^+}[H^+] \ll D_{HCO_3^-}[HCO_3^-] \tag{21}$$

$$D_{OH^-}[OH^-] \ll D_{CO_3^=}[CO_3^=] \tag{22}$$

$$D_{OH^-}[OH^-] \ll D_{HCO_3^-}[HCO_3^-] \tag{23}$$

The formal errors in the diffusion coefficients made adopting the approximations in Eqs. (16), (17) and (19) can be as high as a factor of two (see Table 1); however, an error of this size does not propagate to the solutions. Solutions to linear diffusion problems exhibit square-root functionalities on diffusivity, and this attenuated dependency continues in nonlinear problems. In addition, HCO_3^- is far and away the most abundant carbonate species, so that diffusion coefficient errors in the CO_2 and $CO_3^=$ equations don't have a significant effect. The inequalities in Eqs. (20) through (21) are quite accurate over the pH range of interest (i.e. 6–8.5). Overall, we are confident that the ease of solution gained by these approximations vastly outweighs the numerical errors they generate.

With the assumptions given above, a simplified system of equations can be generated. For oxygen and sulfate,

$$\frac{\partial[O_2]}{\partial t} = D_{O_2}\nabla^2[O_2] - \frac{138}{106}\frac{R_0 e^{-ax}[O_2]}{K_{O_2} + [O_2]} - 2K_{OS}[O_2][TS] \tag{24}$$

$$\frac{\partial[SO_4]}{\partial t} = D_{SO_4}\nabla^2[SO_4] - \frac{1}{2}\left(\frac{R_0 e^{-ax}[SO_4]}{K_{SO_4} + [SO_4]}\right)\left(\frac{K_p}{K_p + (O_2)}\right) + K_{OS}[O_2][TS] \tag{25}$$

respectively. Also, from the sum of Eqs. (3), (4) and (5),

$$\frac{\partial[TC]}{\partial t} = D_{HCO_3^-}\nabla^2[TC] + \left(\frac{R_0 e^{-ax}[O_2]}{K_{O_2} + [O_2]}\right) + \left(\frac{R_0 e^{-ax}[SO_4]}{K_{SO_4} + [SO_4]}\right)\left(\frac{K_p}{K_p + [O_2]}\right) \tag{26}$$

from the sum of Eqs. (6) and (7),

$$\frac{\partial[TS]}{\partial t} = D_{H_2S}\nabla^2[TS] + \frac{1}{2}\left(\frac{R_0 e^{-ax}[SO_4]}{K_{SO_4} + [SO_4]}\right)\left(\frac{K_p}{K_p + [O_2]}\right) - K_{OS}[O_2][TS] \tag{27}$$

Table 1. Parameter values for oxygen-sulfide-pH model. Initial concentrations are standard seawater values. Porosity was assumed constant with depth, and the bottom flux through the base of the tube and the base of the chamber was set to zero.

I. Initial Values C_i			
$[O_2]$	0.00025 M	$[SO_4]$	0.028 M
$[TCO_2]$	0.0022 M	pH	8.0
II. Monod Constants and Equilibrium Constants			
K_{O_2}	1×10^{-5} (M)†	K_{C1}	1.053×10^{-6} (M)§
K_{SO_4}	1.5×10^{-3} (M)#	K_{C2}	6.418×10^{-10} (M)§
K_p	1×10^{-5} (M)	K_S	1.89×10^{-7} (M)§
		K_W	1.537×10^{-14} (M^2)§
III. Free Solution Diffusion Coefficients ($cm^2\ min^{-1}$) (corrected for temperature)			
H^+	4.08×10^{-3} §	$CO_3^=$	3.754×10^{-4} §
OH^-	2.116×10^{-3} §	$SO_4^=$	4.235×10^{-4} §
O_2	8.523×10^{-4} §	H_2S	7.332×10^{-4} §
CO_2	7.189×10^{-4} §	HS^-	7.36×10^{-4} §
HCO_3^-	4.406×10^{-4} §		
IV. Rate Constants			
Heterogeneous reaction rate R_0		1.0×10^{-5} ((M min^{-1})	
Sulfide oxidation rate constant K_{OS}		0.0, 0.006, 0.012 (M^{-1} min^{-1})	
V. Additional Parameters			
Porosity		0.85	
Depth Attenuation Coefficient a (cm^{-1})		0.0	
Bottom Flux $B\left(\frac{\partial C}{\partial x} = B \text{ at } x = L, x = L_1\right)$		0.0	
Temperature (°C)		11.0	

†From Devol, 1974.
#From Boudreau and Westrich, 1984.
§From Boudreau and Canfield, 1993.

and from the sum of Eqs. (4), 2× (5), (7) and −(8),

$$\frac{\partial [TA]}{\partial t} = D_{HCO_3^-} \nabla^2 [TA] + \left(\frac{R_0 e^{-ax} [SO_4]}{K_{SO_4} + [SO_4]}\right)\left(\frac{K_p}{K_p + [O_2]}\right) - 2K_{OS}[O_2][TS] \tag{28}$$

where

$$[TC] = [CO_2] + [HCO_3^-] + [CO_3^=] \tag{29}$$

$$[TS] = [H_2S] + [HS^-] \tag{30}$$

$$[TA] = [HCO_3^-] + 2[CO_3^=] \tag{31}$$

b. Boundary conditions and parameter values. The boundary conditions and initial condition for this type of model are described and justified extensively in Boudreau and Marinelli (1994). Only a brief review and illustration (Fig. 2) is given here. We assume that,

at the sediment-water interface and for each solute,

$$C = C_0 \qquad x = 0 \tag{32}$$

where C_0 is a known constant concentration of the solute in question. At the edge of the annulus,

$$\frac{\partial C}{\partial r} = 0 \qquad r = r_2 \tag{33}$$

where r_2 = outer radius of the sediment annulus (Fig. 2). Eq. (33) states that there is no diffusive flux of solute across the outer surface of the sediment annulus in the radial direction. Another identical annulus is assumed to exist on the other side of the surface so that the concentration field is a mirror image on the other side (Aller, 1980). The model assumes reactions can continue in sediments below the cylinder, so that a flux of solute is permitted:

$$\frac{\partial C}{\partial x} = B \qquad x = L_1 \tag{34}$$

where L_1 = axial length of the sediment annulus being modeled.

During periods of irrigation, we specify that the solute concentration within the tube and at the tube-sediment boundary is known constant and the same as the overlying water:

$$C = C_0 \qquad r = r_1 \text{ and } x \leq L \tag{35}$$

where r_1 = radius of the irrigated tube (Fig. 2). During the quiescent nonirrigation periods, the concentration of a given solute within the tube water ($0 \leq r \leq r_1$, $0 \leq x \leq L$) is governed by a simplified equation of the form:

$$\frac{\partial C}{\partial t} = D_S \frac{\partial^2 C}{\partial x^2} + \frac{D_s}{r} \frac{\partial}{\partial r}\left(r \frac{\partial C}{\partial r}\right) \tag{36}$$

i.e. solutes within the tube can diffuse, but no reactions occur within the tube itself, and where D_S is a generic porewater diffusion coefficient. Consequently, across the tube-sediment interface, we assume that concentrations are continuous in the r-direction:

$$(C(x \leq L, r_1, t))^+ = (C(x \leq L, r_1, t)) \tag{37}$$

with a change in the gradient given by

$$\left(\varphi 0^{-2} \left.\frac{\partial C}{\partial r}\right|_{r1}\right)^+ = \left(\left.\frac{\partial C}{\partial r}\right|_{r1}\right)^- \qquad (x \leq L). \tag{38}$$

At the base of the irrigated tube, the concentration is continuous

$$(C(x = L, 0 \leq r \leq r_1, t))^+ = (C(x = L, 0 \leq r \leq r_1, t))^- \tag{39}$$

while the gradient is again discontinuous

$$\left(\varphi\theta^{-2}\frac{\partial C}{\partial x}\bigg|_L\right)^+ = \left(\frac{\partial C}{\partial x}\bigg|_L\right)^- \qquad (0 \leq r \leq r_1) \tag{40}$$

where θ is the tortuosity, φ is the porosity of the sediment (assumed constant) and the superscripts + and − indicate that a boundary is approached from larger or smaller values of x or r. Crossing the centerline, $r = 0$, the concentration is symmetrical in any radial direction, so:

$$\frac{\partial C}{\partial r}\bigg|_{r=0} = 0. \tag{41}$$

The initial condition specifies that solute values within sediments are the same as in the overlying water:

$$C = C_i \qquad t = 0 \tag{42}$$

where C_i is determined either by direct measurement or from the literature (Table 1).

The resulting model was solved by operator-splitting (the locally 1-D method) and explicit finite differences (for details of this numerical method see Nogotov, 1978; Mitchell and Griffiths, 1980; Lapidus and Pinder, 1982; Ramos, 1986). The model was run for 10 days of model time, after which the initial transient had decayed, and in the periodically irrigated case, the concentration distributions at each step in the irrigation/nonirrigation cycle were identical regardless of which cycle was examined. Our model was capable of examining solute profiles at any time during the irrigation cycle. We chose as a benchmark to examine profiles 55 minutes subsequent to the initiation of the irrigation cycle.

The initial concentrations, Monod constants, equilibrium constants, rate constants and diffusion coefficients for the solutes and reactions, and additional parameter values are listed in Table 1. An upper limit on the reaction rate R_0 was calculated from the oxygen profile from control experiments. (We had hoped to use the sulfate profile, but technical difficulties prevented this.) Specifically, because our sediments were completely mixed at the beginning of the experiment, we assumed that there was no depth attenuation of the decay with depth, i.e. $a = 0$. Therefore, if the steady state one-dimensional O_2-profile in the control sediments is due solely to organic matter oxidation (which is not quite true), then the diagenetic equation for the oxygen is (Bouldin, 1968)

$$\frac{d^2[O_2]}{dx^2} - R_0' \approx 0 \tag{43}$$

where $R_0' \equiv R_0/D_{O2}$, for which the solution is

$$[O_2] \approx \frac{R_0' x^2}{2} + Ax + B \tag{44}$$

where A and B are unknown integration constants. The depth, x_0, where O_2 disappears is treated as an unknown by Bouldin (1968), who introduces three boundary conditions to resolve the indeterminacy, i.e.

$$[O_2](x = 0) = C_0 \tag{45}$$

$$[O_2](x = x_0) = 0 \tag{46}$$

$$\left.\frac{d[O_2]}{dx}\right|_{x=x_0} = 0 \tag{47}$$

The value of x_0 is not, however, an unknown in our case, as it can be determined from observation.

Eq. (44) can be combined with Eqs. (45) through (47) to solve for A, B and R_0'. After minor algebraic manipulations, one obtains

$$[O_2] \approx C_0(x/x_0 - 1)^2 \tag{48}$$

and, as a result,

$$R_0 \approx R_0' D_{O_2} = \frac{2D_{O_2}C_0}{x_0^2} \tag{49}$$

We fully realize that Eq. (49) must produce, at best, an upper limit on the rate of O_2 consumption by organic matter, as part, and maybe all, the O_2 demand is by oxidation of sulfide (Boudreau and Canfield, 1993). Nevertheless, the need to produce some limit on R_0 necessitated this treatment. Eq. (49) tells us that if values of x_0 and C_0 from the non-irrigated controls are substituted into this equation, R_0 values can calculated. x_0 varied from 0.02 to 0.07 cm, and C_0 varied from 20 to 84 μM; thus, R_0 had an upper range of 3.1 to 31 μM min^{-1}.

We varied the model values of the irrigation cycle to reflect the conditions in our experiment: 5 min irrigation/55 min no irrigation, 20 min irrigation/40 min no irrigation, 60 min irrigation/0 min no irrigation. Boundary perturbations with these periodicities, t_p, will be "felt" a distance, l, into the sediment given by Einstein's relation,

$$l = \sqrt{2D_s t_p}. \tag{50}$$

The calculated l values are only a few millimeters at most; thus a fine submillimeter grid, at least near the boundary, is needed to resolve the effects of these phenomenon. Because the

method of calculation is an explicit finite difference scheme, this fine grid places significant limits on the time step. (We also experimented with implicit finite difference methods, but they were slower even with larger time steps.)

To determine the potential importance of sulfide oxidation to the model-predicted sulfide, pH and oxygen profiles, model runs were conducted with three values of the sulfide oxidation constant K_{OS}, as given in Table 1. We had no measurements to fix this constant, and we were interested only in the largest possible effect. Consequently, the chosen K_{OS} values reflect the largest values of this constant for which the numerical method remains stable. These are calculated by the requirement that

$$K_{OS} < \frac{0.1 D_{O_2}}{r_1^2 [SO_4^=]_0} \tag{51}$$

where $[SO_4^=]_0$ is the sulfate concentration at the sediment-water interface.

4. Laboratory results

During the initial 10-day equilibration period, a two-layer oxic/anoxic sediment column developed. While larger fauna were successfully excluded from the sieved sediments, a number of smaller organisms (e.g. copepods, nematodes, polychaetes) populated the surface sediments and in some cases constructed small burrows or tubes (<1 cm diameter and <1.5 cm deep). These fauna created substantial small-scale heterogeneity in surficial sediments, but did not perturb the larger gradients imposed by the 15 cm irrigated tube.

a. Oxygen. Sediments in the experimental and control core became progressively more anoxic, as indicated by the depth of the oxic layer, over the course of the experiment (Fig. 3). Within a given measurement period, oxygen concentrations in both cores were variable, presumably due to the small-scale mixing and irrigation activities of meiofauna and smaller macrofauna. During the first irrigation cycle (5 minute irrigation/55 minute no irrigation), oxygen microelectrode measurements revealed oxygen penetration into sediments of less than 0.15 mm (Fig. 3). By the end of the experiment, both experimental and control cores harbored small patches of *Beggiatoa*-like bacterial mats, and oxygen penetration into sediments was generally <0.1 mm (Fig. 3). Water column oxygen concentration fluctuated, ranging between 40 and 250 μM, during the irrigation cycle, presumably due to high sediment oxygen demand and natural variation in oxygen levels in the seawater system source water (Northwest Arm). There was no compelling evidence that more frequent irrigation resulted in sustained increases in oxygen concentration in sediments, even close to the tube wall (Fig. 3). Presumably, oxygen consumption rates were sufficiently high that any additional oxygen reaching sediments was consumed immediately.

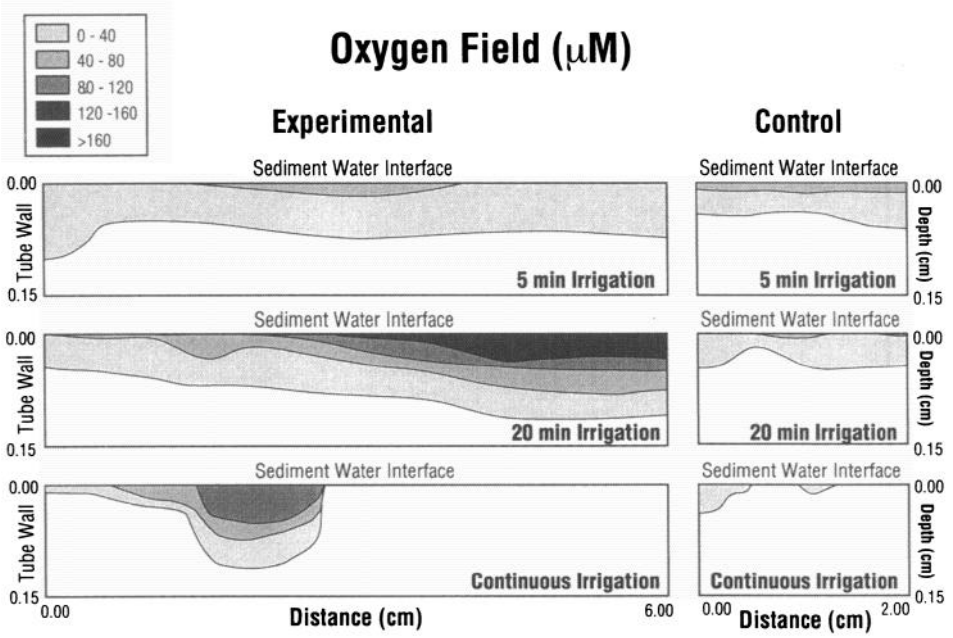

Figure 3. A contour plot of oxygen concentrations in sediments adjacent to the irrigated tube, and in controls, for the 5 minute, 20 minute and continuous irrigation trials. In all cases, the depth of oxygen penetration was shallow (<0.15 cm), and decreased over the course of the experiment. No additional oxygen was detected in sediment surrounding the tube as a function of the duration of irrigation. In controls, the depth of oxygen penetration was somewhat variable, due to the activities of smaller (<350 μm diameter) fauna.

b. pH. Sediment pH values in experimental and control sediments were initially very low (Fig. 4). In control sediments, the initial pH field, measured at the conclusion of the 5 minute irrigation trial, was in the 6.0–6.6 pH range (Fig. 4 top). Near the top of the sediment column, pH began to rise but never reached the overlying water value of 8.0. (Values in the top 1–2 mm are not shown because, in most cases, the pH gradient is steep relative to the scale of the graph, and labelling of all values would render the top portion unreadable.)

The pH field in the control core at the time of the 20 minute irrigation period indicates an increase in pH values over time (Fig. 4 middle). A small region near the sediment surface was characterized by pH values in the 6.0–6.5 range, but the majority of the sediment pH was between 6.6–6.7. At the conclusion of the continuous irrigation period, pH in controls was not very different from that observed at the end of the 20 minute irrigation (Fig. 4 bottom). pH ranged from 6.6–6.7 in the 0–2.0 cm depth range, with a slight rise to 6.8–6.9 in the 3–4 cm depth range. The relatively small-scale variation in pH values in the control core may be due to some patchiness in sediments, but the variation seems to diminish over the course of the experiment.

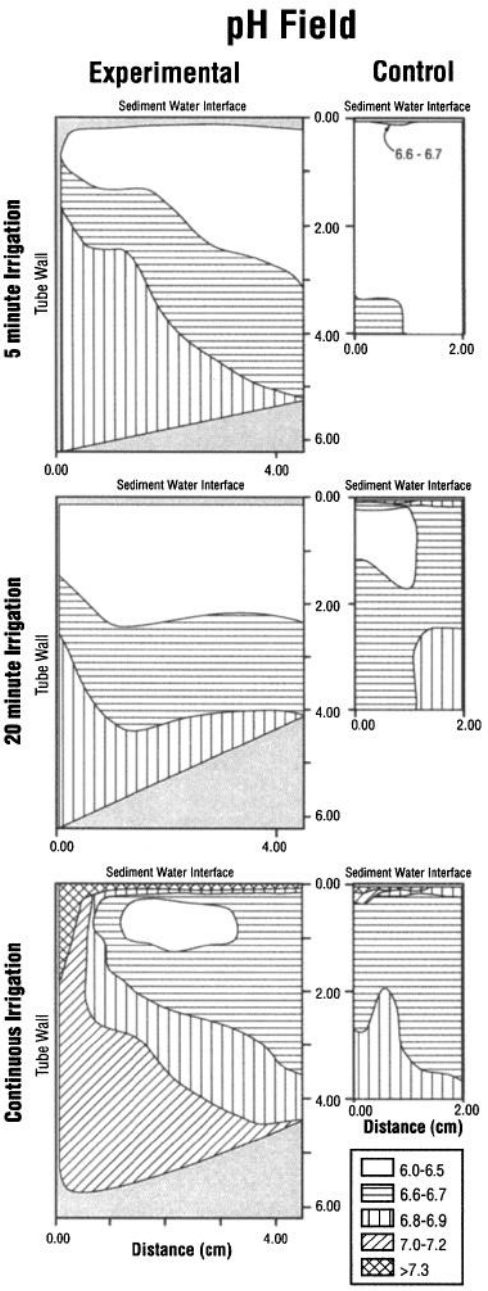

Figure 4. A contour plot of the pH field in control and experimental sediments at the conclusion of the 5 minute, 20 minute and continuous irrigation trials. In both cores, pH gradually increased over the duration of the experiment. In irrigation cores, the influence of overlying water pH is most evident when sediments are continuously irrigated.

In the experimental core, the influence of tube irrigation on the pH field was evident for all irrigation cycles, with marked differences as a function of irrigation frequency. At the conclusion of both the 5 minute and 20 minute irrigation runs, sediment pH showed similar values as in controls, but the pH contours slope upward toward the tube, indicating higher pH's close to the tube wall (Fig. 4 top and middle). pH values were not obtained directly at the tube-sediment interface, as such a measurement may have broken the probe. The influence of tube irrigation on sediment pH values extended one to several centimeters away from the tube edge into the sediment. In sediments relatively far from the tube (e.g. 4 cm), pH values were similar to controls (Fig. 4).

For continuous irrigation, more striking results were obtained. Sediment pH values rose dramatically within several cm of the tube edge, denoting a strong overlying water influence (Fig. 4 bottom). Farther from the tube, (>3.0 cm) sediment pH's resembled those in controls measured at the same point in time (Fig. 4 bottom). These results suggest that in general, the control sediments and the experimental sediments far from the irrigated tube exhibited similar changes over the course of the experiment. Thus, the differences observed in sediment qualities close to the tube can be attributed to variation in irrigation frequency, as opposed to natural variation.

5. Model calculations

Before presenting the results from the model calculations, we wish to stress again that the model is not an accurate simulation of the experimental system. Ammonium, iron and manganese species are absent from the model, in part to keep computational times to a reasonable duration (i.e. at most a day or two per run). Also, there are transients in the real data that are not duplicated in the model, such as the long-term changes in O_2 in the overlying waters and the net (unquantified) loss of organic matter during the course of the experiment. Nevertheless, the modeling results are informative.

The oxygen-sulfide-pH model was run with the same irrigation frequencies used in the experiments and with several different values of sulfide oxidation (Table 1). Model predictions of oxygen concentrations in sediments subjected to 5 minute irrigation, with no sulfide oxidation, suggest some penetration of oxygen into the sediment. However, the majority of the oxygen gradient falls within the tube (Fig. 5a). During continuous irrigation (no sulfide oxidation), the oxygen contours are shifted and significantly compressed, indicating an extremely steep gradient at the tube-sediment boundary (Fig. 5b). Model results for 20 minute irrigation are intermediate between 5 minute and continuous irrigation predictions and are not shown.

To more adequately depict the differences between the predicted oxygen field for 5 minute versus continuous irrigation, the percent difference between the two fields was calculated. Highest percentages were observed in the sediment region immediately adjacent to the tube, with a lateral decay in the signal over a short (mm) spatial scale (Fig. 5c). The potential importance of sulfide oxidation can be appreciated by comparing the predicted oxygen field for continuous irrigation with and without sulfide oxidation

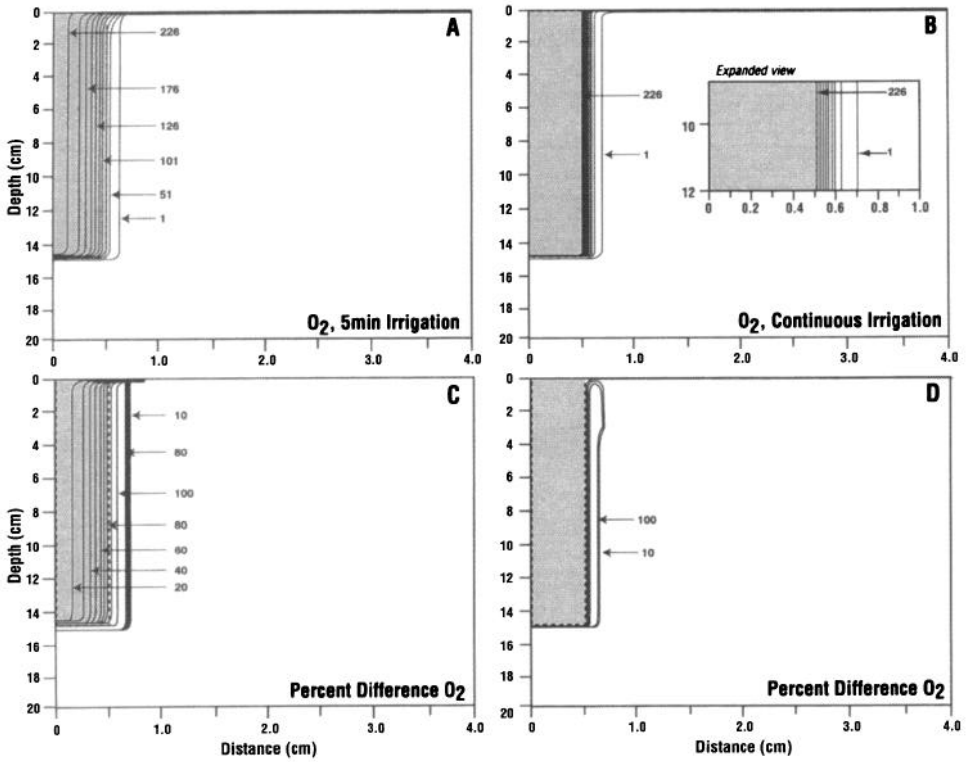

Figure 5. Model-predicted effects of irrigation on oxygen gradients in sediments. (A) Results for 5 minute irrigation and (B) results for continuous irrigation, for an irrigated tube of radius 0.5 cm, a surrounding sediment domain of radius 4.0 cm and no sulfide oxidation. Concentrations are in μM, and the contour interval for (A) and (B) is 50 μM. (C) The percent difference in the oxygen concentration field for 5 minute vs. continuous irrigation with no sulfide oxidation. (D) The percent difference in the predicted oxygen concentration field for continuously irrigated sediments with and without sulfide oxidation, for $r_1 = 0.5$, $r_2 = 4.0$ and tube length = 15 cm. For (C) and (D), the contour interval is 10%.

(maximum value of 0.012, Table 1). This condition maximizes the amount of oxygen available for sulfide oxidation and is, therefore, an "endmember" case. Percent differences in the oxygen field for this comparison show a potentially large effect of sulfide oxidation on oxygen concentrations, with differences as high as 100 percent (Fig. 5d). As in the previous examples, the difference was confined to sediments close (~mm) to the tube.

Model predictions of total sulfide (ΣH_2S) concentrations in irrigated sediments imply a substantial irrigation effect on the sulfide field and extremely high sulfide levels (27 mM, nearly complete conversion of sulfate to sulfide) in regions far from the tube (Fig. 6a and b). This trend was evident for the 5 minute (Fig. 6a), 20 minute (not shown) and continuous irrigation (Fig. 6b) concentration fields. During continuous irrigation, a slight shift of sulfide contours away from the tube indicates lower predicted concentrations close to the

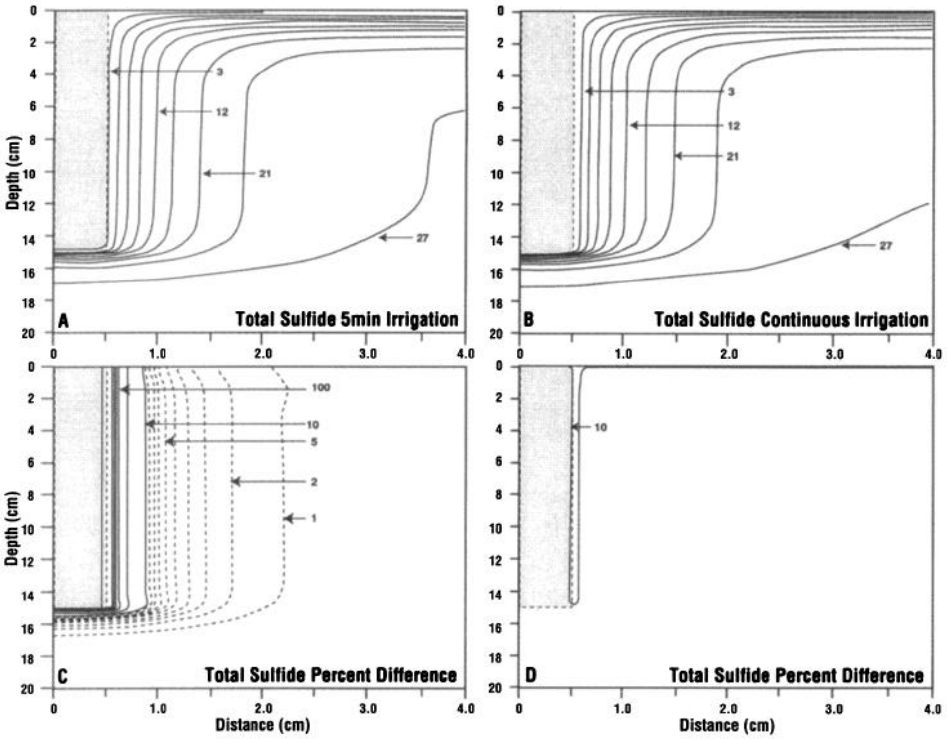

Figure 6. Model-predicted effects of irrigation on total sulfide (ΣH_2S, HS^- and $S^=$) gradients in sediments. (A) Results for 5 minute irrigation and (B) results for continuous irrigation, for an irrigated tube of radius 0.5 cm, a surrounding sediment domain of radius 4.0 cm and no sulfide oxidation. Concentrations are in mM, and the contour interval for (A) and (B) is 3 mM. (C) The percent difference in the total sulfide concentration field for 5 minute vs. continuous irrigation with no sulfide oxidation. Contours with solid lines have intervals of 10%, contours with dashed lines have intervals of 1%. (D) The percent difference in the predicted sulfide concentration field for continuously irrigated sediments with and without sulfide oxidation, for $r_1 = 0.5$ and $r_2 = 4.0$. Contour interval is 10%.

tube wall (Fig. 6b). Unlike oxygen concentration contour lines, sulfide concentration contours were not "compressed" with increasing duration of irrigation (Fig. 6b).

Calculations of the percent difference in the sulfide field for 5 minute versus continuous irrigation indicate the largest impact of irrigation frequency occurs within 3 mm of the tube (Fig. 6c). Unlike oxygen, however, the calculated percent difference extends well into the sediment (2.0 cm from tube wall). The predicted sulfide field for continuous irrigation with and without sulfide oxidation (maximum value of 0.012, Table 1) shows a very slight effect of sulfide oxidation on sulfide concentrations (Fig. 6d). This probably is due to a small amount (micromolar) of oxygen available for oxidation relative to a large amount (millimolar) of total sulfide in surrounding sediments.

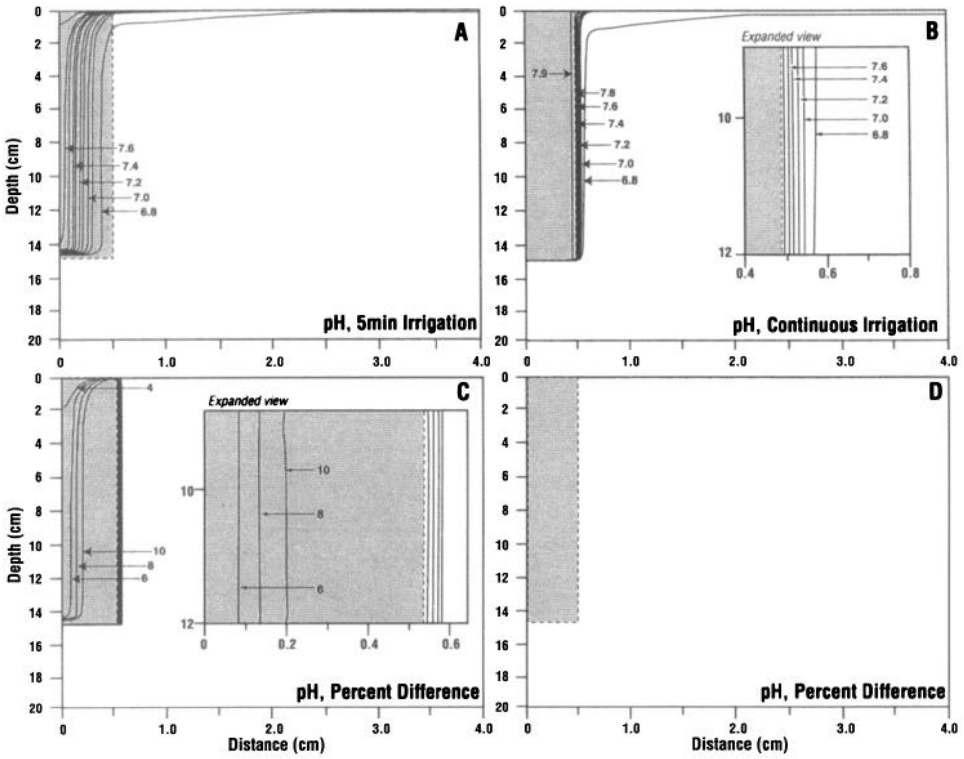

Figure 7. Model-predicted effects of irrigation on pH gradients in sediments. (A) Results for 5 minute irrigation and (B) results for continuous irrigation, for an irrigated tube of radius 0.5 cm, a surrounding sediment domain of radius 4.0 cm and no sulfide oxidation. For (A) and (B), the contour interval is 0.1 pH units. (C) The percent difference in the pH concentration field for 5 minute vs. continuous irrigation with no sulfide oxidation. The contour interval is 2%. (D) The percent difference in the predicted pH field for continuously irrigated sediments with and without sulfide oxidation, for $r_1 = 0.5$ and $r_2 = 4.0$. The influence of sulfide oxidation is sufficiently small that differences > than 2% are not observed.

Model predictions of pH values for the 5 minute irrigation frequency suggest that all pH gradients should fall within the tube, i.e. the sediment pH field is completely homogeneous with pH = 6.8 (Fig. 7a). For continuous irrigation, pH gradients extend from the tube boundary into sediments, but the gradient decays within 2 mm of the tube wall (Fig. 7b). Calculations of percent difference in the pH field for 5 minute vs. continuous irrigation show the region of greatest difference lies within the tube (Fig. 7c). However, we note that the percent difference quantity for pH is somewhat artifactual, as pH is measured on a logarithmic scale. Sulfide oxidation, which liberates protons, did not significantly affect model predictions of pH (i.e. no detectable percent difference with the highest level of sulfide oxidation permitted, Fig. 7d). The concentration of protons liberated during sulfide oxidation was insufficient to shift pH as little as 0.1 pH units.

6. Discussion

Irrigation is an important process in nearshore sediments, facilitating greater exchange between sediments and seawater and imparting significant heterogeneity to the porewater profiles of many constituents. Our combined experimental and modeling study examines the extent to which irrigation and its frequency, a species-specific trait, affect fine-scale gradients in sediments surrounding irrigated tubes. While the model is capable of representing the small-scale concentration fluctuations accompanying transient behaviors (e.g. the 1-hour irrigation cycle), the experimental data are averaged over a longer period of time (3–5 hours/measurement period/electrode) and cannot capture such detail. However, the temporal variation in predicted profiles for zeroth-order reactions within a given irrigation cycle is small (Boudreau and Marinelli, 1994). Thus, any differences between model-predicted and observed concentrations are undoubtedly valid throughout the entire irrigation cycle.

If irrigation frequency has significant effects on solute distributions in bioturbated habitats, one would expect to see differences in the solute fields generated in the experimental and model study. In fact, both the experimental data and the model-generated results predict differences in one or more of the measured variables (oxygen, sulfide and pH) as a function of irrigation frequency (Figs. 3 through 7); however, the two approaches are at variance with respect to the nature and extent of the irrigation-related differences. For oxygen, the model predicts sharper gradients and increasing penetration of oxygen into sediments with additional irrigation (Fig. 5). However, the laboratory data indicated no marked oxygen penetration into sediments as irrigation increased (Fig. 3). For pH, the model predicts sharp pH gradients across the tube-sediment boundary with a virtually homogeneous pH field in the sediments surrounding the tube (Fig. 7). On the other hand, the laboratory sediments were characterized by much lower pH values than the model sediments, with irrigation-driven gradients spread over a larger horizontal scale in the irrigated core (Fig. 4). These results suggest that (1) some model parameters do not reflect true experimental values and/or (2) additional reactions occurred in the experimental sediments that were not contained in the model.

a. Experiment vs. model results—oxygen. Several possibilities may have caused the variance in oxygen concentrations between the measured sediment values and model predictions. First, the actual rate of organic matter oxidation for the entire sediment column may have been higher than that entered into the model. This is unlikely, given the high sulfide concentrations predicted by the model (Fig. 6), and the fact that the organic matter oxidation rate was estimated as a maximum from laboratory oxygen profiles.

Secondly, the overlying water oxygen concentration used in the model was often greater than that observed in the experiment, i.e. fluctuating boundary condition in the experiment vs. a static boundary condition in the model. Thus, less oxygen would be available to sediments immediately surrounding the tube, resulting in low or no oxygen in sediments adjacent to the tube wall. Low and variable overlying water concentrations were partly due

to high sediment oxygen demand, combined with greater exchange of overlying water during tube irrigation, as well as to variations in Dalhousie's seawater system. Finally, it is possible that, along the tube wall or in sediments immediately surrounding the tube, reactions were different from, or reaction rates were higher than in the model. Thus, upon entry into sediments, additional oxygen was consumed at a faster rate, or more likely, by a different process. This implies the assumption of a homogeneous reaction field or rate for the entire sediment domain in the model may be erroneous.

b. Experiment vs. model results—pH. The low pH values in experimental and control sediments relative to the predicted model values (Fig. 4) are a bit puzzling. The initial pH was uniform and quite low in the experimental and control cores, most likely due to oxidation of the dissolved sulfide, i.e. reactions (VII) and (VIII) above, during sieving and homogenization of the sediment. In addition, there may have been significant oxidation of ammonia and reduced dissolved iron and manganese, which releases protons and drives down the pH, i.e.,

$$NH_4^+ + 2O_2 + 2HCO_3^- \rightarrow NO_3^- + 2H^+ + 3H_2O \quad (52)$$

$$4Fe^{2+} + O_2 + 6H_2O \rightarrow 4FeOOH + 8H^+ \quad (53)$$

$$2Mn^{2+} + O_2 + 2H_2O \rightarrow 2MnO_2 + 4H^+ \quad (54)$$

With time, however, pH rises in both cores, and this general trend of rising pH results from more than one process. Certainly there is a flux of hydrogen ion out of the sediments, but this may be a relatively minor component. Reactions (53) and (54), if they occurred, may be reversed, consuming hydrogen ions. More important, sulfate reduction (reaction II) resumes. This reaction produces more alkalinity (HCO_3^-) than acid (H_2S and HS^-), which buffers the system towards a value dictated by the first dissociation constant of carbonic acid, i.e. near 6.8 (Boudreau and Canfield, 1988, 1993). This is exactly the pH level seen in the control cores at the end of the experiments (Fig. 4). The sulfide produced by sulfate reduction will also react with any metal oxides and/or oxy-hydroxides to raise the pH, e.g. from Boudreau and Canfield (1988),

$$2FeOOH + HS^- + 5H^+ \rightarrow 2Fe^{2+} + 4H_2O + S^0 \quad (55)$$

and, from Burdige and Nealson (1986),

$$MnO_2 + H_2S + 2H^+ \rightarrow Mn^{2+} + 2H_2O + S^0 \quad (56)$$

Yet, despite these hydrogen-ion consuming reactions, an intense pH minimum zone (6.0–6.5) persists for a surprisingly long time in the irrigated cores. We are somewhat at a loss to explain the persistence of this feature. The localized formation of iron monosulfide,

i.e.

$$Fe^{2+} + HS^- \rightarrow 2FeS + H^+ \tag{57}$$

would lead to a lowering or maintenance of low pH, but there is no obvious reason why this reaction should be concentrated in this particular zone. In addition, the net effect of sulfide removal by reaction with iron oxyhydroxides and precipitation of FeS is to raise the pH, as shown by Boudreau and Canfield, (1993). Furthermore, the minimum does not appear to be related to the oxidation of sulfide with oxygen, i.e. reactions (VII) and (VIII), as Figure 3 shows that O_2 does not penetrate that far into the sediment. Finally, it is unlikely that this is due to an inappropriate value of R_0.

The model also does not reproduce the same type of pH minimum observed in the cores. The model predicts that the pH should become homogeneous only a short distance from either the sediment-water interface or the tube wall. To produce the type of minimum seen in the data, one can run a model with a depth-dependent rate of sulfate reduction, $a \neq 0$; this easily obtains a minimum zone of the same form, but not one of this unusual strength, i.e. minimum pH < 6.6. The homogenization of our sediments, however, argues strongly against this depth-dependent effect. Obviously, there is more to the details of pH control in anoxic sediments than we now understand.

c. Implications for natural systems. While we have suggested a number of mechanisms for the discrepancies between the laboratory and model results, we regard the model primarily as a framework for interpreting the data and revealing additional processes that warrant further study in the laboratory and field. Thus, our model is a simplification of the laboratory study, but equally important, the laboratory study is a simplification of nature. In the field, sedimentary conditions are rarely homogeneous, and boundary conditions in bioturbated sediments, like those of Eastern Passage, are more likely to be transient than steady. Moreover, the Eastern passage site, like many intertidal and subtidal mudflats, is characterized by an assemblage of organisms, ranging from deep-dwelling frequent irrigators (e.g. *Arenicola marina*) to more shallow-dwelling quiescent infauna (e.g. relatively surficial spionids), whose activities vary on time scales of hours (e.g. feeding activity) to days (movements of burrows and tubes). These assemblages create a myriad of geochemical environments, undoubtedly driven in part by species-specific differences in irrigation frequency. These differences may be magnified with changes in the sediment organic content. Model runs of periodic irrigation suggest that gradients of oxygen, sulfide and pH are more laterally spread and more significantly affected by periodic irrigation when organic matter oxidation rates (a proxy for sediment organic content) are lower, but still sufficient to promote sulfate reduction.

If differences in irrigation behavior can produce local variation in porewater conditions and diagenetic processes, then the behaviors of individual irrigating organisms can have significant effects on geochemical and biological processes in sediments. For example, if

conditions at the tube/sediment interface are transient as a result of irrigation, then decomposition at the tube-sediment boundary may be strongly linked to irrigation frequency. Moreover, if porewater conditions local to tubes (e.g. within 2–3 cm) are influenced by irrigation behavior, then distributions of bacteria, meiofauna, and macrofauna may be similarly affected. Future studies of irrigation should examine the dependence of ecological and geochemical phenomena near irrigated dwellings on the behavior of individuals, as well as the interactions among organisms, in bioturbated habitats.

Acknowledgments. We thank Barry Hargrave, Jon Grant and Brian Schofield for use of their equipment, Ed Berman and Stuart Levine (at Diamond General) for advice on the use of microelectrodes, Tom Gross for assistance with Matlab, and the Skidaway graphics department for preparation of figures. We also thank R. C. Aller and two anonymous reviewers for constructive comments on an earlier draft. This research was supported by grants from DFO Canada, DEMR Canada, NSERC (Canadian Joint Global Ocean Flux program) and NSF (OCE93-14681).

REFERENCES

Aller, R. C. 1977. The influence of macrobenthos on chemical diagenesis of marine sediments. Ph.D. dissertation, Yale University, 600 pp.

—— 1978. Experimental studies of changes produced by deposit feeders on pore water, sediment, and overlying water chemistry. Am. J. Sci., *278,* 1185–1234.

—— 1980. Quantifying solute distributions in the bioturbated zone of marine sediments by defining an average microenvironment. Geochim. Cosmochim. Acta, *44,* 1955–1965.

—— 1982. The effects of macrobenthos on chemical properties of marine sediment and overlying water, *in* Animal Sediment Relations. P. L. McCall and M. J., Tevesz, eds., Plenum Press, NY.

—— 1983. The importance of the diffusive permeability of animal burrow linings in determining marine sediment chemistry. J. Mar. Res., *41,* 299–322.

—— 1994a. Bioturbation and remineralization of sedimentary organic matter: effects of redox oscillation. Chem. Geol., *114,* 331–345.

—— 1994b. The sedimentary Mn cycle in Long Island Sound: Its role as intermediate oxidant and the influence of bioturbation, O_2 and C_{org} flux on diagenetic reaction balances. J. Mar. Res., *52,* 259–295.

Aller, R. C. and J. Y. Yingst. 1985. Effects of the marine deposit-feeders *Heteromastus filiformis* (Polychaeta), *Macoma balthica* (Bivalvia), and *Tellina texana* (Bivalvia) on averaged sedimentary solute transport, reaction rates and microbial distributions. J. Mar. Res., *43,* 615–645.

Berner, R. A. 1980. Early Diagenesis. Princeton University Press, Princeton, NJ, 241 pp.

Boudreau, B. P. 1987. A steady-state diagenetic model for dissolved carbonate species and pH in the porewaters of oxic and suboxic sediments. Geochim. Cosmochim. Acta, *51,* 1985–1996.

—— 1991. Modelling the sulfide-oxygen reaction and associated pH gradients in porewaters. Geochim. Cosmochim. Acta, *55,* 145–159.

Boudreau, B. P. and D. E. Canfield. 1988. A provisional diagenetic model for pH in anoxic porewaters: Application to the FOAM Site. J. Mar. Res., *46,* 429–455.

—— 1993. A comparison of closed- and open-system models for porewater pH and calcite-saturation state. Geochim. Cosmochim. Acta, *57,* 317–334.

Boudreau, B. P. and R. L. Marinelli. 1994. A modelling study of discontinuous biological irrigation. J. Mar. Res., *52,* 947–968.

Boudreau, B. P. and J. T. Westrich. 1984. The dependence of bacterial sulfate reduction on sulfate concentration in marine sediments. Geochim. Cosmochim. Acta, *48,* 2503–2516.

Bouldin, D. R. 1968. Models for describing the diffusion of oxygen and other mobile constituents across the mud-water interface. J. Ecol., *56,* 77–87.

Burdige, D. J. and K. H. Nealson. 1986. Chemical and microbial studies of sulfate-mediated manganese reduction. Geomicrobiol. J., *4,* 361–387.

Canfield, D. E., B. Thamdrup and J. W. Hanse. 1994. The anaerobic degradation of organic matter in Danish coastal sediments: Iron reduction, manganese reduction and sulfate reduction. Geochim. Cosmochim. Acta, *57,* 3867–3883.

Dales, R. P. 1961. Oxygen uptake and irrigation of the burrow by three terebellid polychaetes: *Eupolymnia, Thelepus,* and *Neoamphitrite.* Physiol. Zool., *34,* 306–311.

Dales, R. P., C. P. Mangum and J. C. Tichy. 1970. Effects of changes in oxygen and carbon dioxide concentrations on ventilation rhythms in Onuphid polychaetes. J. Mar. Biol. Assoc. U.K., *50,* 365–380.

Devol, A. H. 1975. Biological oxidation in oxic and anoxic marine environments, rates and processes. Ph.D., University of Washington, Seattle, 208 pp.

Emerson, C. W. and J. Grant. 1991. The control of soft-shell clam (*Mya arenaria*) recruitment on intertidal sandflats by bedload sediment transport. Limnol. Oceanogr., *36,* 1288–1300.

Forster, S. and G. Graf. 1992. Continuously measured changes in redox potential influenced by oxygen penetrating from burrows of *Callianassa subterranea.* Hydrobiologia., *235/236,* 527–532.

Hargrave, B. T. and G. A. Phillips. 1981. Annual *in situ* carbon dioxide and oxygen flux across a subtidal marine sediment. Estuar. Coast. Shelf Sci., *12,* 725–737.

Krager, C. D. and S. A. Woodin. 1993. Spatial persistence and sediment disturbance of an arenicolid polychaete. Limnol. Oceanogr., *38,* 509–520.

Kristensen, E. 1983. Ventilation and oxygen uptake by three species of *Nereis* (Annelida: Polychaeta). I. Effects of hypoxia. Mar. Ecol. Prog. Ser., *12,* 289–297.

Kristensen, E., R. C. Aller and J. Y. Aller. 1991. Oxic and anoxic decomposition of tubes from the burrowing sea anemone *Cerianthiopsis americanus:* Implications for bulk sediment carbon and nitrogen balance. J. Mar. Res., *49,* 589–617.

Kristensen, E. and T. H. Blackburn. 1987. The fate of organic carbon and nitrogen in experimental marine sediment systems: Influence of bioturbation and anoxia. J. Mar. Res., *45,* 231–257.

Lapidus, L. and G. F. Pinder. 1982. Numerical Solution of Partial Differential Equations in Science and Engineering, John Wiley and Sons, NY, 677 pp.

Mangum, C. P. 1964. Activity patterns in metabolism and ecology of polychaetes. Comp. Biochem. Physiol., *11,* 239–256.

Marinelli, R. L. 1992. Effects of polychaetes on silicate dynamics and fluxes in sediments: Importance of species, animal activity and polychaete effects on benthic diatoms. J. Mar. Res., *50,* 745–779.

—— 1994. Effects of burrow ventilation on activities of a terebellid polychaete and silicate removal from sediment porewaters. Limnol. Oceanogr., *39,* 303–317.

Martin, W. R. and G. T. Banta. 1992. The measurement of sediment irrigation rates: A comparison of the Br-tracer and $^{222}Rn/^{226}Ra$ disequilibrium techniques. J. Mar. Res., *50,* 125–154.

Meyers, M. B., E. N. Powell and H. Fossing. 1987a. Microdistribution of interstitial meiofauna, oxygen and sulfide gradients, and the tubes of macroinfauna. Mar. Ecol. Prog. Ser., *35,* 233–241.

—— 1987b. Movement of oxybiotic and thiobiotic meiofauna in response to changes in porewater oxygen and sulfide gradients around macroinfaunal tubes. Mar. Biol., *98,* 395–414.

Mitchell, A. R. and D. F. Griffiths. 1980. The Finite Difference Method in Partial Differential Equations, John Wiley and Sons, NY, 272 pp.

Monod, J. 1949. The growth of bacterial cultures. Ann. Rev. Microbiol., *3,* 371–394.

Nogotov, E. F. 1978. Applications of Numerical Heat Transfer. Hemisphere Publishing Corporation, UNESCO, Paris, 142 pp.

Rabouille, C. and J.-F. Gaillard. 1991. A coupled model representing the deep-sea organic carbon mineralization and oxygen consumption in surficial sediments. J. Geophys. Res., *96,* 2761–2776.

Ramos, J. I. 1986. Numerical solution of reaction-diffusive systems. Part 3: Time linearization and operator splitting techniques. Inter. J. Comp. Math., *18,* 289–309.

Van Cappellen, P., J.-F. Gaillard and C. Rabouille. 1993. Biogeochemical transformations in sediments: kinetic models of early diagenesis, *in* Interactions of C, N, P, and S Biogeochemical Cycles and Global Change, R. Wollast, F. T. Mackenzie and L. Chou, eds., NATO ASI Series v. 14.

Wells, G. P. 1949. Respiratory movements of *Arenicola marina* L.: Intermittent irrigation of the tube, and intermittent aerial respiration. J. Mar. Biol. Assoc. U.K., *28,* 447–464.

Wells, G. P. and R. P. Dales. 1951. Spontaneous activity patterns in animal behaviour: The irrigation of the burrow in the polychaetes *Chaetopterus variopedatus* Renier and *Neries diversicolor.* O. F. Muller. J. Mar. Biol. Assoc. U.K., *29,* 661–680.

Wheatcroft, R. A., I. Olmez and F. X. Pink. 1994. Particle bioturbation in Massachusetts Bay: Preliminary results using a new deliberate tracer technique. J. Mar. Res., *52,* 1129–1150.

Winer, R. J. 1971. Statistical Principles in Experimental Design, McGraw-Hill, NY, 907 pp.

Woodin, S. A. 1984. Effects of browsing predators: Activity changes in infauna following tissue loss. Biol. Bull., *166,* 558–573.

—— 1985. Effects of defecation by Arenicolid polychaete adults on spionid polychaete juveniles in field experiments: selective settlement or differential mortality. J. Exp. Mar. Biol. Ecol., *87,* 119–132.

Received: *24 August 1995;* revised: *12 June, 1996.*